Grunwald and Weber *Computational Urban Science* (2021) 1:25
https://doi.org/10.1007/s43762-021-00026-7

Computational Urban Science

ORIGINAL PAPER Open Access

Influence of urban land-use change on cold-air path occurrence and spatial distribution

Laura Grunwald* and Stephan Weber

Abstract

The urban population is predicted to reach a 70% share of global population by mid-century. Future urbanization might be directed along several development typologies, e.g. sprawling urbanization, more compact cities, greener cities, or a combination of different typologies. These developments induce urban land-use change that will affect urban climate and might reinforce phenomena such as the urban heat island and thermal discomfort of urban residents. A planning-based mitigation approach to ensure thermal comfort of residents are urban cold-air paths, i.e. low-roughness areas enabling drainage and transport of colder air masses from rural surroundings. We study how urban land-use change scenarios influence cold-air path occurrence probability and spatial distribution in a mid-European city using a machine learning approach, i.e. boosted regression trees. The Urban Sprawl Scenario results in the strongest reduction of cold-air path area by 3.6% in comparison to the reference case. The Green City Scenario gives evidence for an increase of cold-air path area (2.2%) whereas the Compact Green City Scenario partly counteracts the negative influence of urban densification by increased fractions of vegetated areas. The proposed method allows for the identification of priority areas for cold-air path preservation in urban planning.

Keywords: Urban cold-air paths, Machine learning, Urban climate, Land-use change, Urban development

1 Introduction

Global urbanization is projected to further increase the urban population by about 1.2 billion people by 2030 with a likely expansion of urban land area by 1.2–1.8 million km^2 between 2000 and 2030 (McDonald et al., 2020; Seto and Pandey, 2019). However, despite the urbanization process on a global scale, a city is constantly developing and transforming on the local scale (Mahtta et al., 2019; Tonne et al., 2021). These processes might be triggered by economic prosperity or economic decline, a growing or shrinking urban population and by different municipal planning concepts, e.g. more sustainable urban design. Different typologies of urban growth and development might be distinguished such as

- urban sprawl, in which built-up areas expand towards the urban periphery increasing the low residential housing density (mainly conversion from agricultural to urban land use; Bart, 2010; EEA, 2016; Neuman, 2005; Oueslati et al., 2015),
- compact cities, in which vacant plots are developed and urban expansion is directed vertically resulting in a higher population density (Daneshpour and Shakibamanesh, 2011; Gaigné et al., 2012; Neuman, 2005, Mahtta et al., 2019)
- green cities, in which the share of green infrastructure such as parks and pocket parks, green roofs and facades increases (Lafortezza et al., 2013; Lin et al., 2017)

* Correspondence: l.grunwald@tu-bs.de
Climatology and Environmental Meteorology, Institute of Geoecology, Technische Universität Braunschweig, Langer Kamp 19c, 38106 Braunschweig, Germany

- compact green cities, which are a combination of compact city and green city development (Artmann et al., 2019; Richter and Behnisch, 2019)
- shrinking cities, which are mainly characterized by urban decline for different reasons such as population loss or deindustrialization (Li and Xie et al., 2018, Galster, 2019).

Urban development results in changes of land-use mainly with conversion of natural surfaces into artificial surface types. These processes modify the urban atmosphere and might reinforce phenomena such as the urban heat island (UHI, Huang et al., 2019; Jato-Espino, 2019; Manoli et al., 2019) which is projected to intensify with global warming due to more frequent heat waves and hot summer nights (e.g. Doan et al., 2019; Wouters et al., 2017). Higher urban temperatures will increase the bioclimatic burden and mortality of the urban population (e.g. Li et al., 2012; Gabriel and Endlicher, 2011).

Different effects of urban development typologies on meteorological quantities and urban climate phenomena are documented (e.g. Alexander et al., 2016). Urban sprawl with conversion of arable land and reduction of vegetation cover was shown to increase the average urban air temperature in Teheran, Iran, by approximately 1 °C (Emadodin et al., 2016). Generally, sprawling urbanization was reported to be more vulnerable to extreme heat events than compact cities (Stone et al., 2010). A compact city development is characterized by controlled vertical growth, redevelopment of urban brownfields, large fractions of impervious surfaces, and a high degree of accessibility (Daneshpour and Shakibamanesh, 2011). However, the higher density of compact cities results in limited ventilation by fresh and cold-air (Masoumi et al., 2017; Peng et al., 2017; Tablada et al., 2009, Wang et al., 2018). A higher share of green infrastructure in the green city typology, however, provides urban ecosystem services such as heat mitigation by increased evapotranspiration as well as habitats for different animal species (Grunwald et al., 2017; Lafortezza et al., 2013). Urban parks, forests, street trees, green roofs and facades help to decrease surface and air temperatures (e.g. Heusinger and Weber, 2015; Oberndorfer et al., 2007; Zölch et al., 2016).

Cold-air paths are a planning-based mitigation measure to reduce UHI intensity (e.g. Fahed et al., 2020, Grunwald et al., 2019; He et al., 2020a, b). These are low-roughness areas, which enable drainage and transport of colder air masses from rural surroundings or open spaces into the urban area (Mayer et al., 1994). Cold-air is preferably 'formed' in clear, calm summer nights with low cloud cover and low wind speeds. Cold-air transport via cold-air paths is triggered by thermal urban-rural differences (local pressure differences) or by drainage in hilly terrain due to local buoyancy forces (e.g. Blumen et al., 1999; Mahrt et al., 2001). The occurrence and spatial distribution of cold-air paths depends on different factors. Earlier research indicated that surface elevation height, aerodynamic roughness, and surface land-use such as bare soil, water bodies or green spaces are influencing the occurrence of cold-air paths (e.g. Grunwald et al., 2020; Kuttler et al., 1996; Mayer et al., 1994). Hence, land-use change as caused by urban development may influence morphological and surface properties such as roughness or thermal properties of the surface. This will further affect cold-air production and transport and, consequently, the occurrence and spatial distribution of urban cold-air paths.

However, it is currently understudied to which extent different urban development typologies and associated land-use change may influence cold-air path occurrence and spatial distribution on the urban scale. Hence, a method to predict and quantify this influence would support urban planning and decision-making and help to identify priority areas for cold-air path preservation.

In this study, different scenarios of urban land-use change were applied in a mid-sized German city. We used a machine learning method, that is boosted regression trees (BRT, Elith et al., 2008), to predict the spatial distribution of cold-air paths on the urban scale, which requires less computational time in comparison to numerical modelling. Recently, the method was applied to predict urban cold-air path occurrence in three German cities of different topography (Grunwald et al., 2020). In the present study, the method will be used to study effects of potential future urban land-use change on the occurrence and spatial distribution of cold-air paths. We define four urban land-use change scenarios, i.e. Urban Sprawl, Compact City, Green City and Compact Green City and investigate the possibility to identify priority areas that should remain undeveloped for urban cold-air path preservation.

2 Methods and materials

2.1 Study area

The analysis was conducted in Braunschweig, Northern Germany (52°16′28 N, 10°30′38 E) as a data set of the spatial distribution of cold-air paths was available (Grunwald et al., 2019). Braunschweig has a total surface area of 192 km^2 from which 19.4% are vegetated (park and forest) and 21.9% consist of built-up area. The city has an average building height of 6.4 m, in city center the average building height equals 10.5 m. The lowest surface elevation is 62 m above sea level (asl) in the NW of the city area and the highest elevation is 111 m asl in the SW.

Grunwald et al. (2020) applied and evaluated the method to identify cold-air path occurrence in Braunschweig, Germany. Using observational data they documented higher nocturnal air temperatures in the inner urban area compared to the surroundings, i.e. the urban heat island (c.f. Grunwald et al., 2019). This makes Braunschweig a good test-case to investigate to which extent land-use change by urban development affects cold-air path occurrence.

2.2 Boosted regression tree modelling

To predict cold-air path occurrence and test the influence of different land-use change scenarios we used the method as specified in Grunwald et al. (2020) which is briefly summarized in the following. The machine learning method 'boosted regression trees' (BRT, Elith et al., 2008) was applied to model cold-air path occurrence probability in the study area. To build the BRT model a training data set including information on the relationship of the response variable and the predictor variables is required. The spatial distribution of cold-air paths was used as response variable. The distribution was determined by using the method of Grunwald et al. (2019) who applied the numerical cold-air drainage model KLAM_21 (Sievers, 2005; Sievers and Kossmann, 2016) and geospatial analysis using ArcMap (Version 10.5, Software ArcGIS, ESRI). The vertically integrated heat deficit of the cold-air layer from the KLAM_21 simulation output was used to define cold-air impact regions and cold-air reservoir areas, i.e. areas in which cold-air is accumulated by local-production and/or inflow. Cold-air paths were defined as open areas with low surface roughness, which connect cold air reservoir areas with urban cold-air impact regions. Details of the method are reported in Grunwald et al. (2019). The KLAM_21 model domain for simulating cold-air flow was spatially restricted to the city borders of Braunschweig. Hence, we did not consider the influence of the larger regional scale (e.g. rural surroundings) for cold-air flow. However, KLAM_21 model output was successfully validated with observational data from weather stations and a distributed temperature sensor network that was specifically set up in Braunschweig for model evaluation (Grunwald et al., 2019). This indicates that the influence of the regional scale given the relatively flat topography in the rural surroundings of Braunschweig would not significantly modify the cold-air flow simulation results in the present study.

The occurrence of cold-air paths was available in a binary format estimating either absence (0) or presence of cold-air paths (1) in a horizontal resolution of 100 m. Furthermore, a set of 12 predictor variables was used including surface elevation height difference (ΔDEM), topographic position index (TPI), building volume (BUILDING VOLUME) and nine land-use classes: BUILT_CONTINUOUS, BUILT_DISCONTINUOUS, FOREST, SEMI-SEALED, INDUSTRY, PARK, UNSEALED, SEALED and WATER (cf. Table 1 for details).

To calculate predictor variables, the EU Digital Elevation Model data (EU-DEM) v1.0, Urban Atlas 2012 data available from the European Copernicus Land Monitoring Service and a 3D building model for Braunschweig (kindly provided by the Environmental Agency of the City Administration of Braunschweig) were used. Variables were checked for collinearity using the Spearman's rank coefficient. All correlation coefficients between variable pairs were below a threshold of $|rSpearman| < 0.7$ (Dormann et al., 2013).

The BRT model was built using the package 'dismo' (version 1.1–4, function 'gbm.step', Hijmans et al., 2017) in the R software (R Development Core Team 2018, version 3.5.1). The cold-air path occurrence probability for the city area can be predicted using the 'predict' function in the 'dismo' package. Since all input parameters are based on a horizontal grid-cell resolution of 100×100 m the predicted cold-air path occurrence probability also is grid-cell based. The only difference in comparison to the approach as reported in Grunwald et al. (2020) is that the topographic wind index (TWiI) was not used as a predictor variable. TWiI is thought as a proxy for surface roughness in the built-up area, which potentially limits cold-air flow. It was calculated based on the results of the numerical flow simulation using KLAM_21 (Grunwald et al., 2019; Grunwald et al., 2020). With a modified land-use set-up in the different scenarios new simulation runs would be needed for each modification and would increase computational costs. Model performance of the BRT using TWiI was characterized by a discrimination measure 'area under the receiver operating characteristic curve' of 0.85 (a value of 1.0 indicates a perfect model according to Swets, 1988) whereas the present BRT model (TWiI not included) resulted in a value of 0.84. Hence, TWiI was not taken into account as a predictor to build the BRT model in the present study.

Table 1 Value ranges (median in brackets) of predictor variables ΔDEM (elevation height difference), TPI (topographic position index) and BUILDING VOLUME for Braunschweig. For the nine land-use classes fractions of the total urban area are given. The land-use classes are based on default land-use classes of KLAM_21 (cf. Grunwald et al., 2019)

Predictor variable	Explanation of variable	Value ranges (median)/ Land-use fractions for Braunschweig
ΔDEM (m)	Elevation height difference per grid cell; elevation height of a respective cell minus the minimum elevation height of the city area	0–48 (16)
TPI (m)	mean topographic position index per grid cell; difference between the elevation of a respective cell to the mean elevation of an area of 10,000 m^2 centered around that cell	-15 – 27 (0)
BUILDING VOLUME (m^3)	summed building volume per grid cell	0–40,000 (0)
BUILT_CONTINUOUS (%)	dense built-up area	2.0
BUILT_DISCONTINUOUS (%)	lower-density built-up area	14.9
FOREST (%)	forest area	14.5
SEMI-SEALED (%)	semi-sealed spaces like railroad tracks	1.2
INDUSTRY (%)	built-up area with industry	5.0
PARK (%)	vegetated area with grass, low vegetation and few trees	4.8
UNSEALED (%)	agricultural areas	46.1
SEALED (%)	sealed areas like roads	9.6
WATER (%)	water areas like rivers or lakes	1.9

2.3 Urban land-use change scenarios

Based on different typologies of urban development we defined four scenarios of land-use change to quantify land-use induced modification: 'Urban Sprawl Scenario', 'Compact City Scenario', 'Green City Scenario' and 'Compact Green City Scenario'. We use a conceptual approach, which indicates that the scenarios were not supposed to represent the specifc future development of urban land-use in Braunschweig, e.g. by using detailed municipal land-use plans, but to represent potential typologies of urban future development.

In each scenario current land-use fractions, i.e. the reference case (REF), were modified. To implement the scenarios, four land-use classes taken from the set of BRT predictor variables (c.f. Table 1) were used to define different urban developments, i.e. BUILDING VOLUME, UNSEALED, PARK and BUILT_DISCONTINUOUS. The remaining variables were not considered appropriate to reflect urban development induced land-use change, i.e. topography related parameters such as ΔDEM or TPI are not modified by land-use change. BUILDING VOLUME was taken into account to represent urban growth (e.g. new development areas), or in the case of green city, to analyse the impact of reduced development instead of open green space. In each scenario, 10 steps of land-use modification were applied (Fig. 1). For the 10 steps, land-use fractions were increased linearly to investigate if any sudden leaps or major changes

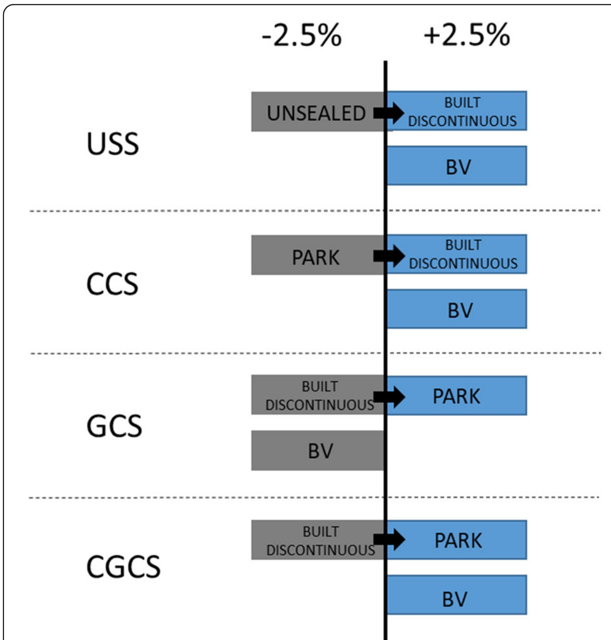

Fig. 1 Land-use modification in the urban development scenarios (USS: Urban Sprawl Scenario, CCS: Compact City Scenario, GCS: Green City Scenario, CGCS: Compact Green City Scenario). In total 10 steps were performed with fixed increments of 2.5% (250 m^2 for land-use and 1000 m^3 for BV (BUILDING VOLUME)

resulted in the model output of cold-air path occurrence.

In the 'Urban Sprawl Scenario' built-up areas (built-up areas defined as areas with BUILDING VOLUME larger than 0 and BUILT_DISCONTINUOUS larger than 0) were defined to spread towards the urban periphery (peripheral areas defined as areas with BUILDING VOLUME equal 0 and BUILT_DISCONTINUOUS equal 0). This is representative for the current situation in Germany which has seen much stronger increase in low density housing during recent decades (i.e. detached housing, single family per house) than higher density housing (Strohbach et al., 2019). Agricultural land-use was converted to built-up area with low residential density. In steps 1–10 the UNSEALED (arable land) land-use adjacent to the built-up area, i.e. a one grid-cell of 100 m resolution, was converted into BUILT_DISCONTINUOUS land-use. To represent a somewhat 'dynamic behavior' in 'Urban Sprawl Scenario' the UNSEALED land-use adjacent to the built-up area was converted into BUILT_DISCONTINUOUS in a larger radius around the built-up area, i.e. a two grid-cell radius of 200 m. Additionally, BUILDING VOLUME increases in increments of 2.5% in these areas. This approach intends to mimic urban densification at the periphery of the built-up area, a process that is typical for new housing development areas in cities (Strohbach et al., 2019). In each step the land-use was modified in linear increments of 2.5%, e.g. the BUILT_DISCONTINUOUS area increased by 250 m^2 per grid-cell whereas the UNSEALED area decreased by 250 m^2 (Fig. 1). BUILDING VOLUME increased by 2.5% of the maximum building volume of the built-up area (i.e. 1000 m^3 as the maximum building volume in Braunschweig amounts to 40,000 m^3, Fig. 1).

In the 'Compact City Scenario' open spaces in the built-up area were converted to high residential density areas. Whereas the 'Urban Sprawl Scenario' grows towards the periphery of the city, the focus of the 'Compact City Scenario' was to achieve compaction of the built-up area. Hence, PARK areas (vegetated areas) were converted to buildings, i.e. PARK surface area was replaced by BUILT_DISCONTINUOUS and BUILDING VOLUME was increased.

In the 'Green City Scenario' the importance of green infrastructure was emphasized by increasing PARK surface area in the built-up area while decreasing BUILT_DISCONTINUOUS and BUILDING VOLUME.

'Compact Green City Scenario' was intended as a mixture of 'Compact City Scenario' and 'Green City Scenario'. Hence, PARK and BUILDING VOLUME were increased with each step whereas BUILT_DISCONTINUOUS was reduced by the same amount.

The definition of different scenarios finally results in a varying spatial distribution of built-up area per grid cell (cf. Fig. 2 and Table 3 in Appendix).

2.4 Quantifying the influence of land-use change on cold-air path occurrence

The BRT model generates cold-air path occurrence probabilities ranging between 0% (no cold-air path) and 100%. The predictions of the BRT model for the four scenarios were compared to REF (cf. section 3.2.1). We analyzed whether the modification of land-use affects the spatial distribution of cold-air paths, i.e. the course of a cold-air path might be either disrupted or it expands to cover a larger surface area. However, in order to analyze cold-air path spatial distribution we needed to set a limit value per grid cell that defines the occurrence of a cold-air path in binary form, i.e. cold-air path either present of absent. This limit value was set according to the cold-air path area given in the BRT model training data, i.e. 60% occurrence probability. Hence, an occurrence probability ≥60% was defined for cold-air

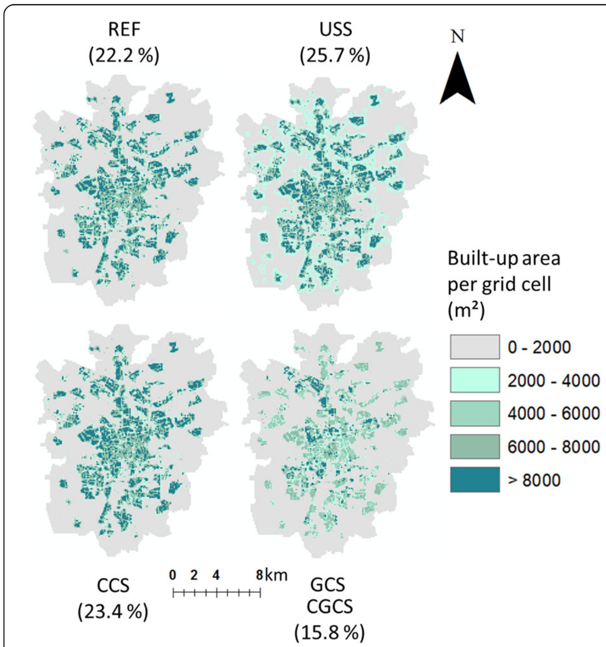

Fig. 2 Built-up area per grid cell (100 × 100 m grid cell) in Braunschweig for the reference case (REF) and for step 10 of the respective scenarios (USS: Urban Sprawl Scenario, CCS: Compact City Scenario, GCS: Green City Scenario, CGCS: Compact Green City Scenario). Step 10 indicates the maximum amount of built-up area, i.e. summed over step 1–10. Additionally, total built-up area is quantified in percent of total urban area (in brackets)

path existence (cf. section 3.2.2). Additionally, four other limit values were tested (50%, 55%, 65% and 75%) to analyze the sensitivity of the limit value on cold-air path occurrence in the different scenarios.

3 Results

3.1 Relative influence of predictor variables

The land-use predictor variables were characterized by different relative influence on BRT output (Table 2). ΔDEM had the greatest effect with a relative influence of 72.6%, followed by BUILDING VOLUME (5.7%) and UNSEALED (5.2%). PARK (1.6%) and BUILT_DISCONTINUOUS (1%) had a lower relative influence. Partial dependence plots (PDP) visualize the influence of a predictor variable on the response variable while accounting for the average effects on all other predictors (Elith et al., 2008). BUILDING VOLUME was characterized by a negative relationship with cold-air path occurrence, i.e. with increasing BUILDING VOLUME the chance of a cold-air path is decreasing (Fig. 3). The variables UNSEALED, PARK, and BUILT_DISCONTINUOUS were characterized by moderate to slight positive relationships.

3.2 Influence of land-use change

3.2.1 Cold-air path occurrence probability

Differences in the occurrence probability of cold-air paths were evident in every urban development scenario (Fig. 4). These mainly occurred in the former built-up area. Both, reduction and increase of areas with cold-air path occurrence were evident.

The 'Urban Sprawl Scenario' was characterized by the largest cold-air path reduction, i.e. 37.9% of the study area showed reduced occurrence probabilities in comparison to REF (Fig. 4). These were mainly located in the city center. However, the occurrence probability in the periphery increased by 7.7%. In the 'Compact City Scenario' the probability of cold-air path occurrence in the study area decreased by 19.5%. The distribution of cold-air path reduction was spatially less confined to specific areas in comparison to 'Urban Sprawl Scenario'. Additionally, the share of areas with increased cold-air path occurrence probabilities was higher than for 'Urban Sprawl Scenario'. 'Green City Scenario' showed the highest increase of occurrence probability with 22.9%. The increase was mainly confined to the city center. 'Compact Green City Scenario' is a combination of 'Compact City Scenario' and 'Green City Scenario' and expressed similar behavior of increased and reduced cold-air path occurrence such as REF. However, the spatial distribution of modification was similar to 'Compact City Scenario'.

Table 2 Relative influence of predictor variables (variables used to define/modify scenarios are marked with #)

Predictor variables	Relative influence (%)
ΔDEM	72.56
BUILDING VOLUME#	5.65
UNSEALED#	5.23
TPI	5.10
WATER	2.63
FOREST	1.97
PARK#	1.56
BUILT_CONTINUOUS	1.48
SEALED	1.03
INDUSTRY	0.99
BUILT_DISCONTINUOUS#	0.95
SEMI-SEALED	0.87

3.2.2 Cold-air path area

Although cold-air path occurrence probability was clearly influenced by land-use change, it has not yet been clarified whether this will also change the spatial distribution of the former cold-air paths (Fig. 5).

In 'Green City Scenario' cold-air path area increased to a total of 2.19% in step 10. Minor peaks were evident step 5 and 8. In 'Urban Sprawl Scenario', however, cold-air path area reduced in all 10 steps, with a pronounced reduction in the first step (2.4%). Subsequently, a small but constant decrease was evident which resulted in a maximum reduction of 3.6% of cold-air path area. 'Compact City Scenario' and 'Compact Green City Scenario' were characterized by total reductions of 2% and 0.8%, respectively. 'Compact Green City Scenario' showed higher cold-air path area than 'Compact City Scenario' for every step. 'Compact City Scenario' and 'Compact Green City Scenario' were marked by a slight increase in step 1 and showed decrease for the remaining steps. All scenarios with an increase of BUILDING VOLUME resulted in a total reduction of cold-air path area.

Due to the increase of built surface area in 'Urban Sprawl Scenario' a loss of cold-air path area especially in the city center, the East, the South and the West of the study area was occurring (Fig. 6, red areas). Cold-air path reduction in these areas was spatially clustered (Figs. 6 and 7, red areas). This indicates that cold-air path areas in these regions were sensitive to increased building development. The former cold-air path in the West of the study area was disrupted, which would prevent further advance of cold-air into the built-up area. In the central area, the strongest reductions of > 80% were clustered adjacent to the city center (Fig. 7, dark

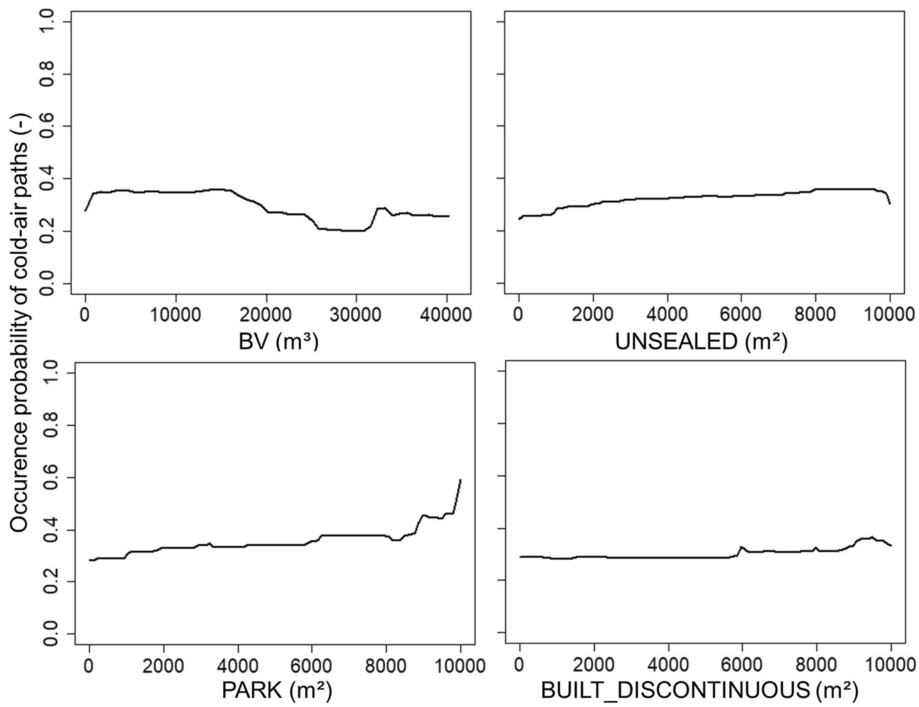

Fig. 3 Partial dependence plots (PDPs) of the variables used for land-use change modification

grey areas). In 'Compact City Scenario' only minor modification in cold-air paths became evident but the reduction was not as spatially concentrated as in 'Urban Sprawl Scenario' (Figs. 6; 7). 'Compact Green City Scenario' showed a very similar spatial distribution of cold-air path reduction. However, the increase of cold-air path area was more prominent in comparison to 'Compact City Scenario' (Fig. 6, green areas; Fig. 8 in the Appendix). In 'Compact City Scenario' and 'Compact Green City Scenario' the spatial distribution of cold-air paths was virtually conserved. Nevertheless, in the city center loss of former cold-air path areas was evident (Fig. 7, dark grey areas).

'Green City Scenario' was characterized by the strongest increase in cold-air path area, especially in the central and eastern parts of the study area (Fig. 6, green areas; Fig. 8 in the Appendix). Generally, a clear increase of spatially connected cold-air path surface area that might have established new cold-air paths did not emerge in any of the four scenarios. Cold-air path reduction was particularly severe in 'Urban Sprawl Scenario' and 'Compact City Scenario' as cold-air was partly prevented from advancing deeper into the built-up area. The cold-air path in the W of 'Urban Sprawl Scenario' was completely disrupted.

Quantification of cold-air path area was based on a limit value of ≥60% for cold-air path occurrence (cf. section 2.4). The sensitivity of using other limit values (50%, 55%, 65% and 70%) was tested, to estimate differences of cold-air path increase and reduction in comparison to the 60% limit value (Fig. 9 in Appendix). The differences were about 1% on average with few outliers. For a limit value of 70%, the largest difference was 3.6% (for 'Urban Sprawl Scenario'). Hence, the sensitivity to different limit values was rather weak.

4 Discussion

4.1 Main influencing predictors of cold-air paths

The elevation height difference is by far the most dominant predictor variable. The largest cold-air path occurrence probabilities occur for low elevation heights, which is plausible as density-driven cold-air drainage accumulates at lower elevation heights (Grunwald et al., 2020; Hjort et al., 2011; Nkemdirim, 1980). Surface elevation differences clearly influences cold-air drainage. Hence, these areas should be identified and preserved. As an example hill slopes, which are prone to cold-air drainage (e.g. Nkemdirim, 1980), are popular settlement areas in many cities. Further residential development and densification in these areas might reduce cold-air supply, i.e. by limiting cold-air production due to sealing of natural surfaces and the increase in roughness by higher building density.

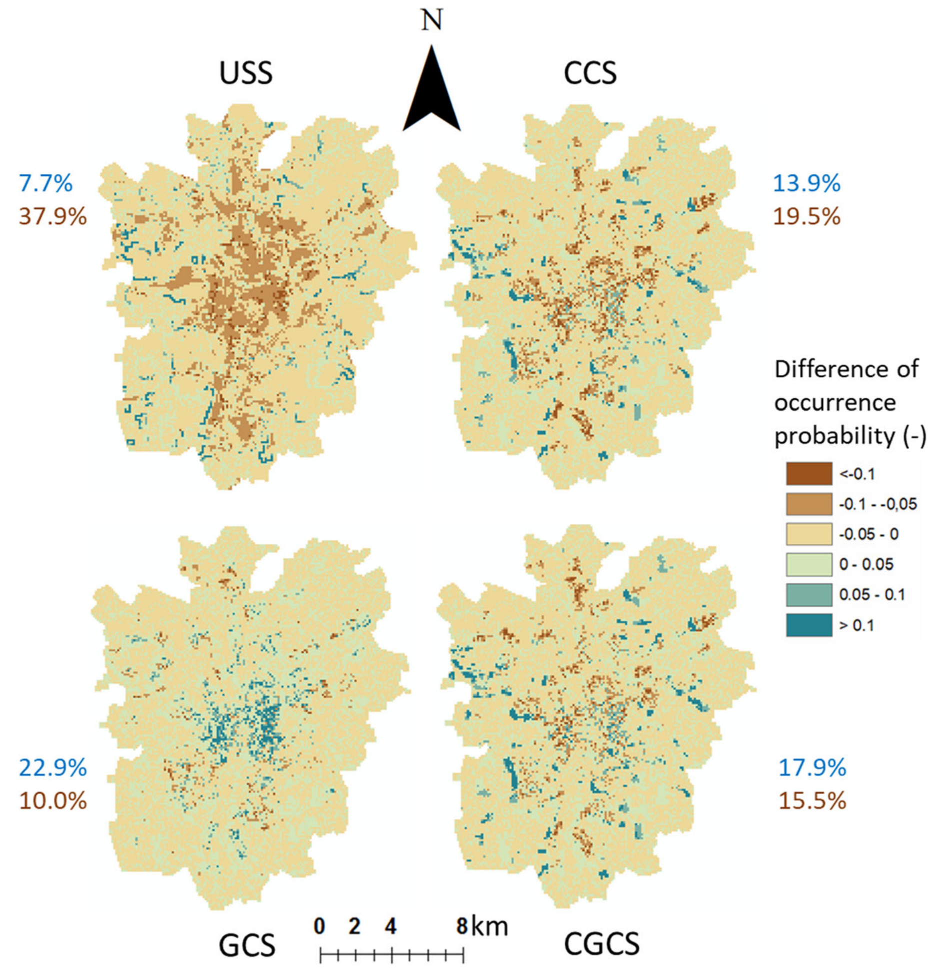

Fig. 4 Average differences of cold-air path occurrence probabilities in the scenarios in comparison to the reference case (= Scenario – REF). The differences were averaged for the 10 steps of land-use modification. Brown colors indicate a reduced probability whereas blue colors indicate an increased probability. The fraction of the study area with increased (blue) or reduced (brown) cold-air path occurrence probabilities is quantified (USS: Urban Sprawl Scenario, CCS: Compact City Scenario, GCS: Green City Scenario, CGCS: Compact Green City Scenario)

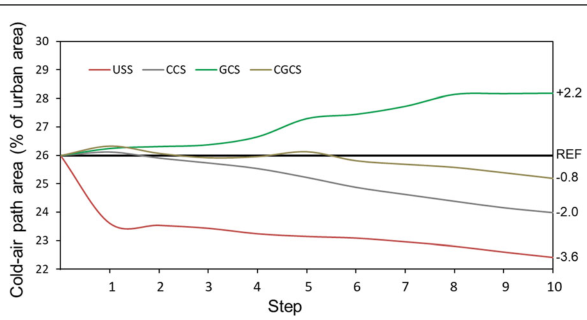

Fig. 5 Cold-air path area variation for the urban development scenarios in 10 steps of land-use modification (USS: Urban Sprawl Scenario, CCS: Compact City Scenario, GCS: Green City Scenario, CGCS: Compact Green City Scenario). The numbers on the right y-axis quantify total variation of cold-air path area at step 10 in comparison to REF (reference case)

Although elevation heights might have the strongest influence on cold-air path occurrence, these are not subject to modification by urban planning. However, land-use is influenced by urban planning and might result in positive or negative effects on cold-air path occurrence. Urban planning processes may influence the variables BUILDING VOLUME and UNSEALED (ranked second and third in relative influence of predictors). The PDPs clearly indicate that further increase of BUILDING VOLUME negatively influences cold-air path occurrence whereas UNSEALED areas preserve cold-air paths. Increased BUILDING VOLUME results in higher aerodynamic roughness, which consequently might suppress cold-air transport (e.g. Goldreich, 1984; Kuttler et al., 1996). The land-use variables UNSEALED and PARK (ranked seventh for relative influence of the predictors) often are low-roughness areas which may produce cold-

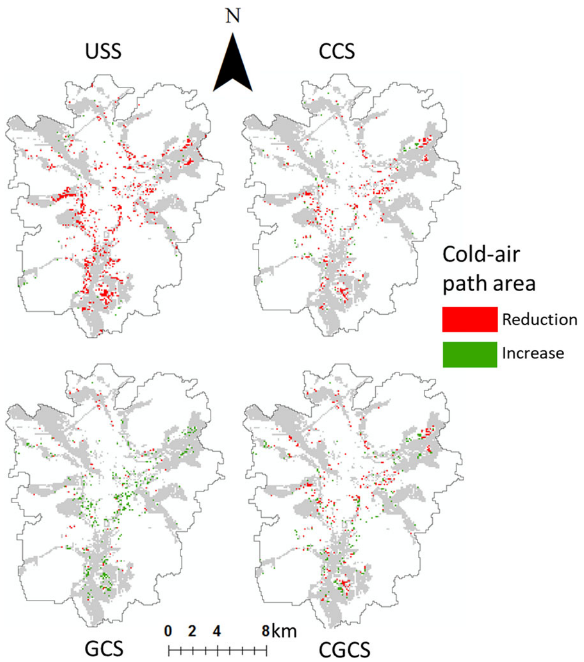

Fig. 6 Cold-air path area (areas with a cold-air path occurrence probability ≥60%) increase (green) and reduction (red) averaged over the 10 steps in comparison to the reference case (lightgrey areas) for the scenarios (USS: Urban Sprawl Scenario, CCS: Compact City Scenario, GCS: Green City Scenario, CGCS: Compact Green City Scenario)

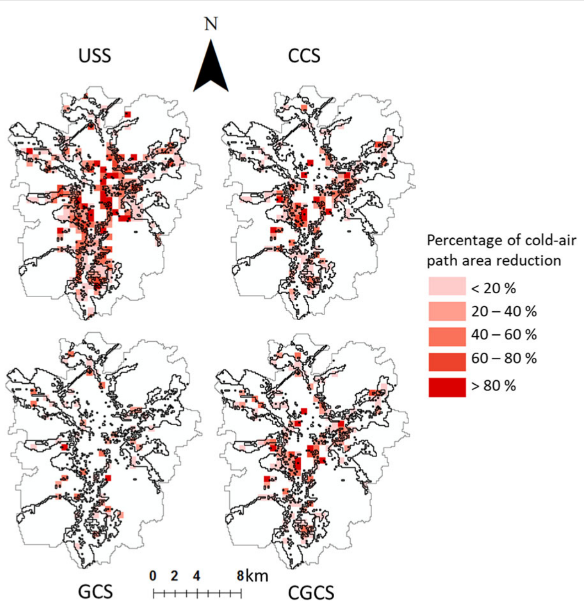

Fig. 7 The percentage of cold-air path area reduction in comparison to the cold-air path area of REF for all scenarios is shown for 500 × 500 m resolution (red scales). For comparison, the outlines of the cold-air paths of REF are shown in black

air (Mayer et al., 1994). Hence, those land-use types should be preserved to promote cold-air production and transport. The slight positive relationship between BUILT_DISCONTINUOUS and cold-air paths was not expected. However, due to an increased degree of surface sealing this land-use type might promote higher nocturnal air temperatures, i.e. urban heat islands. Since cold-air flow might be driven by urban-rural air temperature differences (local pressure differences; e.g. Blumen et al., 1999) this positive relationship is plausible.

4.2 Influence of urban land-use change on cold-air paths

The four development scenarios result in modifications of the occurrence probability and the spatial distribution of cold-air paths. The most distinct changes are evident in 'Urban Sprawl Scenario' with the strongest reduction of cold-air path area in all 10 steps. This is probably due to the modification of UNSEALED and BUILDING VOLUME, which both have a major influence on cold-air path occurrence. In areas with new residential development, an increase in the occurrence probability is evident, which is due to the positive relationship with BUILT_DISCONTINUOUS. In the more densely built-up area, the occurrence probability and spatial distribution of cold-air paths is decreasing. We assume that this is due to the increase in building density, which hinders cold-air dispersion and favors cold-air accumulation at the fringe of the built-up area (Goldreich, 1984; Kuttler et al., 1996). Generally, areas that used to be poorly supplied with cold-air are most strongly affected by land-use modification. Consequently, cold-air paths might be disrupted, e.g. in the W of the study area and the city center. Land-use modification in 'Compact City Scenario' was implemented exclusively within the built-up areas. Areas with higher cold-air path occurrence probability can be identified, in which cold-air is likely to accumulate because of the denser development. 'Compact Green City Scenario' shows a similar spatial distribution of cold-air path modification such as 'Compact City Scenario', however, with limited total reduction of the occurrence probability. The influence of PARK is assumed to compensate for the strong influence of the increase in BUILDING VOLUME, since vegetated areas are prone to cold-air production (Breuste et al., 2013; Oke, 1987). In 'Green City Scenario' the reduced aerodynamic roughness of the built-up area supports cold-air flow (Mayer et al., 1994).

Generally, the cold-air path occurrence probability was most strongly reduced in 'Urban Sprawl Scenario'. This agrees with findings of urban sprawl processes and its influence on different meteorological quantities.

Emadodin et al. (2016) report urban sprawl to result in higher urban air temperature and lower evaporation. Stone et al. (2010) reported more frequently extreme heat events in sprawling metropolitan regions. Further, Mohan et al. (2020) observed higher canopy layer temperatures and reduced thermal comfort due to urban sprawl. 'Compact City Scenario' shows higher cold-air path occurrence and lower cold-air path area reduction than 'Urban Sprawl Scenario'. This is in agreement with results from Stone et al. (2010) who found compact cities to be less vulnerable to extreme heat events than cities characterized by urban sprawl. However, the 'Compact City Scenario' also shows reductions in the total cold-air path area, especially in the city center. This is supported by Lemonsu et al. (2015) who found higher nighttime UHI with increased densification.

The 'Green City Scenario' shows the largest increase of cold-air path occurrence. However, in this scenario the building volume was reduced in favor of green areas. In terms of urbanization and a high need for urban living space in popular cities, options to increase the vegetated surface area are usually scarce. Other solutions such as green roofs and facade greening might be considered (Grunwald et al., 2017; Heusinger and Weber, 2017; Heusinger et al., 2018; Konopka et al., 2021; Oberndorfer et al., 2007). These support cold-air production but not necessarily cold-air transport.

'Compact Green City Scenario' appears to be a promising approach enabling densification through vertically directed urban expansion and growth of the city, while at the same time reducing negative effects on cold-air path occurrence by maintaining areas with lower roughness and greening. Various studies are dealing with the implementation of higher shares of green space in compact cities to reduce urban warming (Haaland and van Den Bosch, 2015; Jim, 2004; Pearsall, 2017; Tian et al., 2012; Wellmann et al., 2020). Trimmel et al. (2019) simulates different urban design concepts and analyses differences in air temperature, surface temperature and thermal comfort. One design concept includes higher densification but also green roofs or optimized material properties. These modifications help to counteract the negative effects of densification. Furthermore, Koch et al. (2018) simulate the redevelopment of an urban brownfield and find that locally adapted planning can minimize the potential warming by denser development.

The present method is able to provide information on the modification of cold-air path occurrence with respect to urban land-use change. Due to the spatial horizontal resolution of 100 m it is not possible to resolve single buildings, e.g. local construction projects cannot be taken into account. However, priority areas for cold-air path preservation that might be kept free from further development are identified.

4.3 Summary and conclusions

Worldwide urban growth has been evident for decades, modifying the land-use of cities and their surrounding areas. This may result in an intensification of urban climate phenomena, such as an increased urban heat island intensity. In order to protect the well-being of urban inhabitants and to avoid health effects due to intensified urban warming, mitigation and adaptation measures have to be taken. Cold-air paths can play an important role in mitigating UHI intensity.

In the present study, the method of Grunwald et al. (2020) was applied to analyze influences on cold-air path occurrence and spatial distribution by defining four urban land-use change scenarios based on different urban development typologies. For this purpose, a BRT model was used to predict the occurrence probabilities of urban cold-air paths for the different scenarios.

In comparison to the reference situation, 'Urban Sprawl Scenario' indicated the largest reduction of total urban cold-air path area. The cold-air path distribution was partly disrupted limiting cold-air flow into denser parts of the urban area. 'Compact City Scenario' showed limited influence on cold-air path occurrence while the spatial distribution was mainly preserved. However, a reduction of cold-air paths in the dense city center was evident in which cold-air supply is most important. 'Green City Scenario' improved cold-air path spatial distribution through the increase of green spaces, which reduce roughness in comparison to built-up areas and might produce cold-air. 'Compact Green City Scenario' could counteract the negative influences of vertically directed densification on cold-air path occurrence to a certain extent by implementing a higher share of low-roughness vegetated area.

The method allows for spatial resolutions ≥100 m, which makes it not feasible for analyzing local construction and planning projects which may need higher spatial resolution. However, is straightforward to identify priority areas for cold-air path preservation. To transfer the method to other locations the robustness of the approach should be tested with data from other cities. These cities are likely to have different topography, morphology or land-use, which may need recalibration of the BRT model.

The proposed method enables prediction of urban land-use change induced influence on cold-air path distribution and allows for the identification of priority areas for cold-air path preservation in urban planning. It might support decision making in analyzing the state and possible future development of urban cold-air paths.

5 Appendix

Table 3 Percentage fraction of land-use in Braunschweig (reference case) and for step 10 of the respective development scenario (USS: Urban Sprawl Scenario, CCS: Compact City Scenario, GCS: Green City Scenario, CGCS: Compact Green City Scenario)

Land-use fractions (% of total urban area)	REF	USS	CCS	GCS	CGCS
BUILT_CONTINUOUS	2.0	2.0	2.0	2.0	2.0
BUILT_DISCONTINUOUS	14.9	17.9	15.7	8.4	8.4
FOREST	14.5	14.5	14.5	14.5	14.5
SEMI-SEALED	1.2	1.2	1.2	1.2	1.2
INDUSTRY	5.0	5.0	5.0	5.0	5.0
PARK	4.8	4.8	4.0	11.3	11.3
UNSEALED	46.1	43.1	46.1	46.1	46.1
SEALED	9.6	9.6	9.6	9.6	9.6
WATER	1.9	1.9	1.9	1.9	1.9

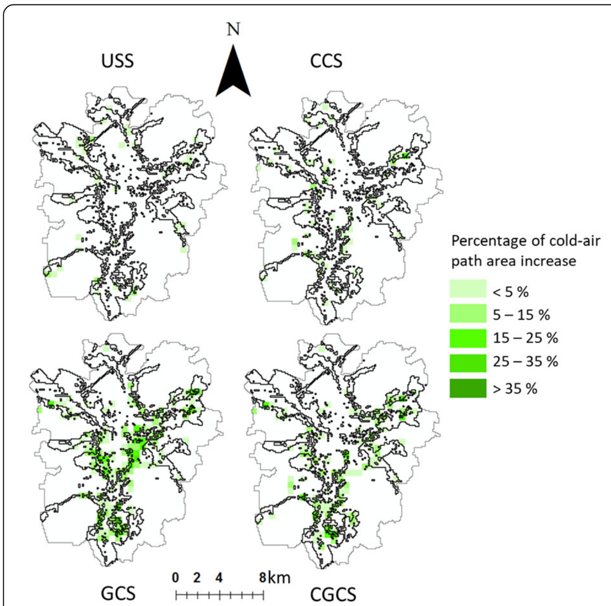

Fig. 8 The clustering of increasing areas is shown through the percentage of cold-air path increase area for all scenarios in comparison to REF for 500 × 500 m horizontal resolution (green scales). Cold-air path surface area of REF is depicted by black lines

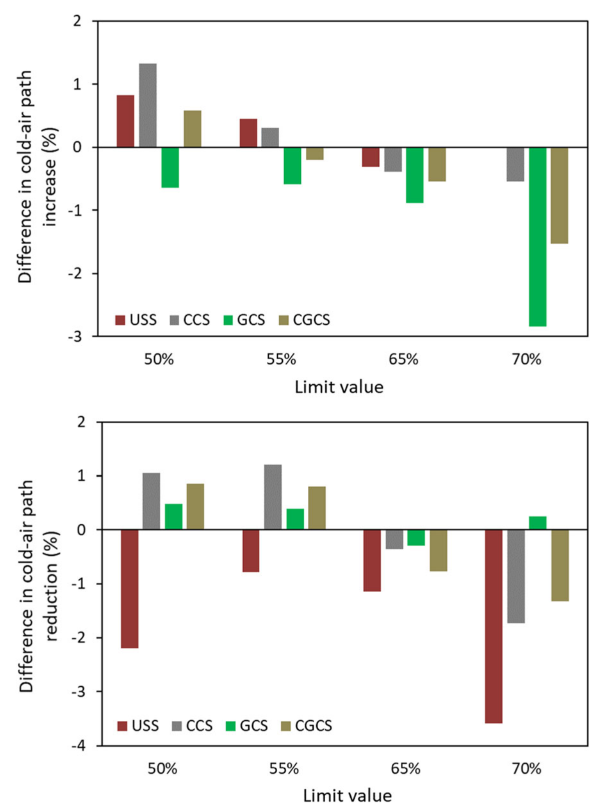

Fig. 9 Differences in cold-air path area increase (top) and reduction (bottom) for the scenarios (USS: Urban Sprawl Scenario, CCS: Compact City Scenario, Green City Scenario, CGCS: Compact Green City Scenario) from the used limit value setting of 60% occurrence probability for the tested limit values of 50%, 55%, 65% and 70%

Acknowledgements
We thank the Lower Saxony Niedersächsisches Vorab for funding the project "METAPOLIS – an inter- and transdisciplinary research platform for the sustainable development of urban-rural relations', funded by the Federal State of Lower Saxony" (Grant No. ZN3121) in which this study was conducted.

Authors' contributions
All authors contributed to the study conception and design. Material preparation, data collection and analysis were performed by Laura Grunwald. The first draft of the manuscript was written by Laura Grunwald and all authors commented on previous versions of the manuscript. All authors read and approved the final manuscript.

Funding
The study was funded by MWK Lower Saxony Niedersächsisches Vorab as part of the collaborative project "METAPOLIS – an inter- and transdisciplinary research platform for the sustainable development of urban-rural relations', funded by the Federal State of Lower Saxony" (Grant No. ZN3121).

Availability of data and materials
The dataset and code generated during the current study are available in the ‚Digital Library – Institutional Repository of the TU Braunschweig', Doi - https://doi.org/10.24355/dbbs.084-202108090856-0 .

Declaration

Competing interests
The authors declare that they have no known competing financial interests or personal relationships that could have appeared to influence the work reported in this paper.

Received: 11 August 2021 Accepted: 29 October 2021
Published online: 19 November 2021

References

Alexander, P. J., Fealy, R., & Mills, G. M. (2016). Simulating the impact of urban development pathways on the local climate: A scenario-based analysis in the greater Dublin region, Ireland. *Landscape and Urban Planning, 152*, 72–89. https://doi.org/10.1016/j.landurbplan.2016.02.006

Artmann, M., Kohler, M., Meinel, G., Gan, J., & Ioja, I. C. (2019). How smart growth and green infrastructure can mutually support each other—A conceptual framework for compact and green cities. *Ecological Indicators, 96*, 10–22. https://doi.org/10.1016/j.ecolind.2017.07.001

Bart, I. L. (2010). Urban sprawl and climate change: A statistical exploration of cause and effect, with policy options for the EU. *Land Use Policy, 27*(2), 283–292. https://doi.org/10.1016/j.landusepol.2009.03.003

Blumen, W., Grossman, R. L., & Piper, M. (1999). Analysis of heat budget, dissipation and frontogenesis in a shallow density current. *Boundary Layer Meteorology, 91*(2), 281–306. https://doi.org/10.1023/A:1001813700928

Breuste, J., Haase, D., & Elmqvist, T. (2013). Urban landscapes and ecosystem services. In S. Wratten, H. Sandhu, R. Cullen, & R. Costanza (Eds.), *Ecosystem services in agricultural and urban landscapes* (pp. 83–104). Wiley. https://doi.org/10.1002/9781118506271.ch6

Daneshpour, A., & Shakibamanesh, A. (2011). Compact city dose it create an obligatory context for urban sustainability? *Iran University of Science & Technology, 21*(2), 110–118.

Doan, V. Q., Kusaka, H., & Nguyen, T. M. (2019). Roles of past, present, and future land use and anthropogenic heat release changes on urban heat island effects in Hanoi, Vietnam: Numerical experiments with a regional climate model. *Sustainable Cities and Society, 47*, 101479. https://doi.org/10.1016/j.scs.2019.101479

Dormann, C. F., Elith, J., Bacher, S., Buchmann, C., Carl, G., Carre, G., Garcia Marquez, J. R., Gruber, B., Lafourcade, B., Leitao, P. J., Münkemüuller, T., Mcclean, C., Osborne, P. E., Reineking, B., Schröder, B., Skidmore, A. K., Zurell, D., & Lautenbach, S. (2013). Collinearity: A review of methods to deal with it and a simulation study evaluating their performance. *Ecography, 36*(1), 27–46. https://doi.org/10.1111/j.1600-0587.2012.07348.x

EEA. (2016). Urban sprawl in Europe. In *Joint EEA-FOEN Report*. Publication Office of the European Union.

Elith, J., Leathwick, J. R., & Hastie, T. (2008). A working guide to boosted regression trees. *Journal of Animal Ecology, 77*(4), 802–813. https://doi.org/10.1111/j.1365-2656.2008.01390.x

Emadodin, I., Taravat, A., & Rajaei, M. (2016). Effects of urban sprawl on local climate: A case study, north Central Iran. *Urban Climate, 17*, 230–247. https://doi.org/10.1016/j.uclim.2016.08.008

Fahed, J., Kinab, E., Ginestet, S., & Adolphe, L. (2020). Impact of urban heat island mitigation measures on microclimate and pedestrian comfort in a dense urban district of Lebanon. *Sustainable Cities and Society, 61*, 102375. https://doi.org/10.1016/j.scs.2020.102375

Gabriel, K. M., & Endlicher, W. R. (2011). Urban and rural mortality rates during heat waves in Berlin and Brandenburg, Germany. *Environmental Pollution, 159*(8-9), 2044–2050. https://doi.org/10.1016/j.envpol.2011.01.016

Gaigné, C., Riou, S., & Thisse, J. F. (2012). Are compact cities environmentally friendly? *Journal of Urban Economics, 72*(2-3), 123–136. https://doi.org/10.1016/j.jue.2012.04.001

Galster, G. (2019). Why shrinking cities are not mirror images of growing cities: A research agenda of six testable propositions. *Urban Affairs review, 55*(1), 355–372. https://doi.org/10.1177/2F1078087417720543

Goldreich, Y. (1984). Urban topoclimatology. *Progress in Physical Geography, 8*(3), 336–364. https://doi.org/10.1177/030913338400800302

Grunwald, L., Heusinger, J., & Weber, S. (2017). A GIS-based mapping methodology of urban green roof ecosystem services applied to a central European city. *Urban Forestry and Urban Greening, 22*, 54–63. https://doi.org/10.1016/j.ufug.2017.01.001

Grunwald, L., Kossmann, M., & Weber, S. (2019). Mapping urban cold-air paths in a central European city using numerical modelling and geospatial analysis. *Urban Climate, 29*, 100503. https://doi.org/10.1016/j.uclim.2019.100503

Grunwald, L., Schneider, A.-K., Schröder, B., & Weber, S. (2020). Predicting urban cold-air paths using boosted regression trees. *Landscape and Urban Planning, 201*, 103843. https://doi.org/10.1016/j.landurbplan.2020.103843

Haaland, C., & van Den Bosch, C. K. (2015). Challenges and strategies for urban green-space planning in cities undergoing densification: A review. *Urban Forestry and Urban Greening, 14*(4), 760–771. https://doi.org/10.1016/j.ufug.2015.07.009

He, B. J., Ding, L., & Prasad, D. (2020a). Relationships among local-scale urban morphology, urban ventilation, urban heat island and outdoor thermal comfort under sea breeze influence. *Sustainable Cities and Society, 60*, 102289. https://doi.org/10.1016/j.scs.2020.102289

He, B. J., Ding, L., & Prasad, D. (2020b). Urban ventilation and its potential for local warming mitigation: A field experiment in an open low-rise gridiron precinct. *Sustainable Cities and Society, 55*, 102028. https://doi.org/10.1016/j.scs.2020.102028

Heusinger, J., Sailor, D. J., & Weber, S. (2018). Modeling the reduction of urban excess heat by green roofs with respect to different irrigation scenarios. *Building and Environment, 131*, 174–183. https://doi.org/10.1016/j.buildenv.2018.01.003

Heusinger, J., & Weber, S. (2015). Comparative microclimate and dewfall measurements at an urban green roof versus bitumen roof. *Building and Environment, 92*, 713–723. https://doi.org/10.1016/j.buildenv.2015.06.002

Heusinger, J., & Weber, S. (2017). Surface energy balance of an extensive green roof as quantified by full year eddy-covariance measurements. *Science of the Total Environment, 577*, 220–230. https://doi.org/10.1016/j.scitotenv.2016.10.168

Hijmans, R. J., Phillips, S., Leathwick, J. & Elith, J. (2017). Species distribution modeling. Documentation on the R package 'dismo', version 1.1–4. Retrieved on august 26th 2019 from https://cran.r-project.org/web/packages/dismo/dismo.pdf. Accessed 26 Aug 2019

Hjort, J., Suomi, J., & Käyhkö, J. (2011). Spatial prediction of urban–rural temperatures using statistical methods. *Theoretical and applied climatology, 106*(1-2), 139–152. https://doi.org/10.1007/s00704-011-0425-9

Huang, K., Li, X., Liu, X., & Seto, K. C. (2019). Projecting global urban land expansion and heat island intensification through 2050. *Environmental Research Letters, 14*(11), 114037. https://doi.org/10.1088/1748-9326/ab4b71

Jato-Espino, D. (2019). Spatiotemporal statistical analysis of the urban Heat Island effect in a Mediterranean region. *Sustainable Cities and Society, 46*, 101427. https://doi.org/10.1016/j.scs.2019.101427

Jim, C. Y. (2004). Green-space preservation and allocation for sustainable greening of compact cities. *Cities, 21*(4), 311–320. https://doi.org/10.1016/j.cities.2004.04.004

Koch, F., Bilke, L., Helbig, C., & Schlink, U. (2018). Compact or cool? The impact of brownfield redevelopment on inner-city micro climate. *Sustainable Cities and Society, 38*, 31–41. https://doi.org/10.1016/j.scs.2017.11.021

Konopka, J., Heusinger, J., & Weber, S. (2021). Extensive urban green roof shows consistent annual net uptake of carbon as documented by 5 years of Eddy-covariance flux measurements. *Journal of Geophysical Research: Biogeosciences, 126*(2). https://doi.org/10.1029/2020JG005879

Kuttler, W., Barlag, A.-B., & Rossmann, F. (1996). Study of the thermal structure of a town in a narrow valley. *Atmospheric Environment, 30*(3), 365–378. https://doi.org/10.1016/1352-2310(94)00271-1

Lafortezza, R., Davies, C., Sanesi, G., & Konijnendijk, C. (2013). Green infrastructure as a tool to support spatial planning in European urban regions. *iForest–biogeosciences and Forestry, 6*(3), 102–108. https://doi.org/10.3832/ifor0723-006

Lemonsu, A., Viguie, V., Daniel, M., & Masson, V. (2015). Vulnerability to heat waves: Impact of urban expansion scenarios on urban heat island and heat stress in Paris (France). *Urban Climate, 14*, 586–605. https://doi.org/10.1016/j.uclim.2015.10.007

Li, B., Sain, S., Mearns, L. O., Anderson, H. A., Kovats, S., Ebi, K. L., Bekkedal, M. Y. V., Kanarek, M. S., & Patz, J. A. (2012). The impact of extreme heat on morbidity in Milwaukee, Wisconsin. *Climatic Change, 110*(3-4), 959–976. https://doi.org/10.1007/s10584-011-0120-y

Li, Y., & Xie, Y. (2018). A new urban typology model adapting data mining analytics to examine dominant trajectories of neighborhood change: a case of metro detroit. *Annals of the American Association of Geographers, 108*(5), 1313–1337. https://doi.org/10.1080/24694452.2018.1433016

Lin, P., Lau, S. S. Y., Qin, H., & Gou, Z. (2017). Effects of urban planning indicators on urban heat island: A case study of pocket parks in high-rise high-density environment. *Landscape and Urban Planning, 168*, 48–60. https://doi.org/10.1016/j.landurbplan.2017.09.024

Mahrt, L., Vickers, D., Nakamura, R., Soler, M. R., Sun, J., Burns, S., & Lenschow, D. H. (2001). Shallow drainage flows. *Boundary Layer Meteorology, 101*(2), 243–260. https://doi.org/10.1023/A:1019273314378

Mahtta, R., Mahendra, A., & Seto, K. C. (2019). Building up or spreading out? Typologies of urban growth across 478 cities of 1 million+. *Environmental Research Letters, 14*(12), 124077. https://doi.org/10.1088/1748-9326/ab59bf

Manoli, G., Fatichi, S., Schläpfer, M., Yu, K., Crowther, T. W., Meili, N., Burlando, P., Katul, G. G., & Bou-Zeid, E. (2019). Magnitude of urban heat islands largely explained by climate and population. *Nature, 573*(7772), 55–60. https://doi.org/10.1038/s41586-019-1512-9

Masoumi, H. R., Nejati, N., & Ahadi, A. A. (2017). Learning from the heritage architecture: Developing natural ventilation in compact urban form in hot-humid climate: Case study of Bushehr, Iran. *International Journal of Architectural Heritage, 11*(3), 415–432. https://doi.org/10.1080/15583058.2016.1238971

Mayer, H., Beckröge, W., & Matzarakis, A. (1994). Bestimmung von stadtklimarelevanten Luftleitbahnen. *UVP-report, 5*, 265–267.

McDonald, R. I., Mansur, A. V., Ascensão, F., Colbert, M.L. , Crossman, K., Elmqvist, T., Gonzalez, A., Güneralp, B., Haase, D., Hamann, M., Hillel, O., Huang, K., Kahnt, B., Maddox, D., Pacheco, A., Pereira, H. M., Seto, K.C., Simkin, R., Walsh, B., Werner, A. S., & Ziter, C. (2020). Research gaps in knowledge of the impact of urban growth on biodiversity. *Nature Sustainability*, *3* (1), 16-24. https://doi.org/10.1038/s41893-019-0436-6

Mohan, M., Sati, A. P., & Bhati, S. (2020). Urban sprawl during five decadal period over National Capital Region of India: Impact on urban heat island and thermal comfort. *Urban climate, 33*, 100647. https://doi.org/10.1016/j.uclim.2020.100647

Neuman, M. (2005). The compact city fallacy. *Journal of Planning Education and Research, 25*(1), 11–26. https://doi.org/10.1177/0739456X04270466

Nkemdirim, L. C. (1980). Cold air drainage and temperature fields in an urban environment: a case study of topographical influence on climate. *Atmospheric Environment, 14*(3), 375–381. https://doi.org/10.1016/0004-6981(80)90071-2

Oberndorfer, E., Lundholm, J., Bass, B., Coffman, R. R., Doshi, H., Dunnett, N., Gaffin, S., Koehler, M., Liu, K. K. Y., & Rowe, B. (2007). Green roofs as urban ecosystems: Ecological structures, functions, and services. *BioScience, 57*(10), 823–833. https://doi.org/10.1641/B571005

Oke, T. R. (1987). *Boundary layer climates*. Methuen & Co Ltd.

Oueslati, W., Alvanides, S., & Garrod, G. (2015). Determinants of urban sprawl in European cities. *Urban Studies, 52*(9), 1594–1614. https://doi.org/10.1177/0042098015577773

Pearsall, H. (2017). Staying cool in the compact city: Vacant land and urban heating in Philadelphia, Pennsylvania. *Applied Geography, 79*, 84–92. https://doi.org/10.1016/j.apgeog.2016.12.010

Peng, F., Wong, M. S., Ho, H. C., Nichol, J., & Chan, P. W. (2017). Reconstruction of historical datasets for analyzing spatiotemporal influence of built environment on urban microclimates across a compact city. *Building and Environment, 123*, 649–660. https://doi.org/10.1016/j.buildenv.2017.07.038

R Develoment Core Team. (2018). R software, version 3.5.1. Available under: https://www.r-project.org/. Accessed 15 Nov 2021

Richter, B., & Behnisch, M. (2019). Integrated evaluation framework for environmental planning in the context of compact green cities. *Ecological Indicators, 96*, 38–53. https://doi.org/10.1016/j.ecolind.2018.05.025

Seto, K. C., & Pandey, B. (2019). Urban land use: Central to building a sustainable future. *One Earth, 1*(2), 168–170. https://doi.org/10.1016/j.oneear.2019.10.002

Sievers, U. (2005). Das Kaltluftabflussmodell KLAM_21. Theoretische Grundlagen, Anwendung und Handhabung des PC-Modells. ISBN 978-3-88148-407-7, Berichte des Deutschen Wetterdienstes Band 227, Frankfurt am Main

Sievers, U., & Kossmann, M. (2016). The cold air drainage model KLAM_21 - model formulation and comparison with observations. *Weather and Climate, 36*, 2. https://doi.org/10.2307/26779385

Stone, B., Hess, J. J., & Frumkin, H. (2010). Urban form and extreme heat events: Are sprawling cities more vulnerable to climate change than compact cities? *Environmental Health Perspectives, 118*(10), 1425–1428. https://doi.org/10.1289/ehp.0901879

Strohbach, M. W., Döring, A. O., Möck, M., Sedrez, M., Mumm, O., Schneider, A.-K., Weber, S., & Schröder, B. (2019). The "hidden urbanization": Trends of impervious surface in low-density housing developments and resulting impacts on the water balance. *Frontiers in Environmental Science, 7*, 29. https://doi.org/10.3389/fenvs.2019.00029

Swets, J. A. (1988). Measuring the accuracy of diagnostic systems. *Science, 240*(4857), 1285–1293. https://doi.org/10.1126/science.3287615

Tablada, A., De Troyer, F., Blocken, B., Carmeliet, J., & Verschure, H. (2009). On natural ventilation and thermal comfort in compact urban environments–the old Havana case. *Building and Environment, 44*(9), 1943–1958. https://doi.org/10.1016/j.buildenv.2009.01.008

Tian, Y., Jim, C. Y., & Tao, Y. (2012). Challenges and strategies for greening the compact city of Hong Kong. *Journal of Urban Planning and Development, 138*(2), 101–109. https://doi.org/10.1061/(ASCE)UP.1943-5444.0000076

Tonne, C., Adair, L., Adlakha, D., Anguelovski, I., Belesova, K., Berger, M., Brelsford, C., Dadvand, P., Dimitrova, A., Giles-Corti, B., Heinz, A., Mehran, N., Nieuwenhuijsen, M., Pelletier, F., Ranzani, O., Rodenstein, M., Rybski, D., Samavati, S., Satterthwaite, D., et al. (2021). Defining pathways to healthy sustainable urban development. *Environment International, 146*, 106236. https://doi.org/10.1016/j.envint.2020.106236

Trimmel, H., Weihs, P., Faroux, S., Formayer, H., Hamer, P., Hasel, K., Laimighofer, J., Leidinger, D., Masson, V., Nadeem, I., Oswald, S. M., Revesz, M., & Schoetter, R. (2019). Thermal conditions during heat waves of a mid-European metropolis under consideration of climate change, urban development scenarios and resilience measures for the mid-21st century. *Meteorologische Zeitschrift, 30*(1), 9–32. https://doi.org/10.1127/metz/2019/0966

Wang, X., Li, Y., Yang, X., Chan, P. W., Nichol, J., & Li, Q. (2018). The street air warming phenomenon in a high-rise compact city. *Atmosphere, 9*(10), 402. https://doi.org/10.3390/atmos9100402

Wellmann, T., Schug, F., Haase, D., Pflugmacher, D., & van der Linden, S. (2020). Green growth? On the relation between population density, land use and vegetation cover fractions in a city using a 30-years Landsat time series. *Landscape and Urban Planning, 202*, 103857. https://doi.org/10.1016/j.landurbplan.2020.103857

Wouters, H., De Ridder, K., Poelmans, L., Willems, P., Brouwers, J., Hosseinzadehtalaei, P., Tabari, H., Vanden Broucke, S., van Lipzig, N. P. M., & Demuzere, M. (2017). Heat stress increase under climate change twice as large in cities as in rural areas: A study for a densely populated midlatitude maritime region. *Geophysical Research Letters, 44*(17), 8997–9007. https://doi.org/10.1002/2017GL074889

Zölch, T., Maderspacher, J., Wamsler, C., & Pauleit, S. (2016). Using green infrastructure for urban climate-proofing: An evaluation of heat mitigation measures at the micro-scale. *Urban Forestry & Urban Greening, 20*, 305–316. https://doi.org/10.1016/j.ufug.2016.09.011

Publisher's Note